

An investigation of the global uptake of CO₂ by lime from 1930 to 2020

Longfei Bing^{1,2,3,*}, Mingjing Ma^{1,4,*}, Lili Liu⁵, Jiaoyue Wang^{1,2,3}, Le Niu^{1,4} and Fengming Xi^{1,2,3}

¹Institute of Applied Ecology, Chinese Academy of Sciences, Shenyang 110016, China

²Key Laboratory of Pollution Ecology and Environmental Engineering, Chinese Academy of Sciences, Shenyang 110016, China

³Key Laboratory of Terrestrial Ecosystem Carbon Neutrality, Liaoning Province, Shenyang 110016, China

⁴University of Chinese Academy of Sciences, Beijing 100049, China

⁵Search CO₂ (Shanghai) Environmental Science & Technology Co., Ltd, Shanghai 200232, China

*:*These authors contributed equally to this work.

10 Correspondence: Fengming Xi (xifengming@iae.ac.cn)

Abstract. A substantial amount of CO₂ is released into the atmosphere from the process of the high temperature decomposition of limestone to produce lime. Due to the high temperature decomposition of limestone in the lime production process, the CO₂ emission in the lime production process is the main contributor to the carbon footprint of the industry. However, during the life cycle of lime production, ~~use and waste disposal~~, the alkaline components in lime will continuously absorb CO₂ in the atmosphere when use and waste disposal. Here, we use-adopt an analytical model describing the carbonation process to obtain regional and global estimates ~~for of the sequestration of carbon uptake~~ from 1963/1930 to 2020 using existing data ~~lime lifecycle~~ use-based material data ~~material during lime life cycle~~. The results reveal that the global uptake of CO₂ by lime increased from 38.259.16 Mt C yr⁻¹ (95-% confidence interval, CI: 27.851.84-51.3818.76 Mt C) in 1930 to 134.3335.27 Mt C yr⁻¹ (95-% CI: 90.3723.63-139.2950.39 Mt C) in 2020. Cumulatively, approximately 4.051444.70 GtC-Mt C (95-% CI: 3.021016.24-5.251961.05 Mt C Gt CO₂) were sequestered by lime produced between 1930 and 2020, and this amount corresponding to 38.798.83% of the process emissions during the same period, mainly contributed from the utilisation stage (58.576.21% ~~to of~~ the total uptake). We also fitted the missing lime output data of China from 1930 to 2001, thus compensating for the lack of China's lime production (cumulative 7023.30 Mt) and underestimation of its carbon uptake (467.85 Mt C) in the international data. Since 1930, lime-based materials in China have accounted for the largest proportion (about 63.95%) of the global total. Our results provide data to support including lime carbon uptake into global carbon budgets and scientific proof for further research of the potential of lime-containing materials in carbon capture and storage. The data utilized in the present study can be accessed at <https://doi.org/10.5281/zenodo.7628614> (Ma, 2023).

25 ~~and China (64.15% of the total uptake).~~ We also fitted the missing lime output data of China from 1930 to 1995, thus compensating ~~making up for the lack of China's lime production (cumulative xx Mt) and underestimation of its carbon uptake (xxx Mt C) of China's lime output by in the international data.~~ Since 1930, Lime-based materials in China has accounted for the

设置了格式: 下标

设置了格式: 下标

设置了格式: 下标

设置了格式: 上标

设置了格式: 字体颜色: 红色

设置了格式: 字体颜色: 红色

设置了格式: 字体颜色: 红色

设置了格式: 字体颜色: 红色

largest proportion of carbon sink, about 63%. Our results provide data support for ~~inclusion of including~~ lime carbon uptake into global carbon budgets and scientific proof for further research of the potential of lime-containing materials in carbon capture and storage technology. The data utilized in the present study can be accessed at <https://doi.org/10.5281/zenodo.7112485> (Ma, 2022)

35 1 Introduction

According to the latest report (6th Assessment) of the Intergovernmental Panel on Climate Change (IPCC), anthropogenic activities are responsible for the unprecedented increase in the concentration of CO₂ in the atmosphere, which ~~attained-reached~~ 415 ppm in 2021 (NOAA. ESRL, 2022). In 2019, approximately 24% (14 Gt CO₂-eq) of the net global anthropogenic emissions originated from industrial sources, and lime production ~~emerged-as-was~~ the second highest industrial source after cement production (IPCC, 2021; Shan et al., 2016). Similar to cement, lime is mainly produced via the heating of limestone (CaCO₃) in a kiln at temperatures of 900–1200 °C. The CO₂ generated during this process is commonly released into the atmosphere (Greco-Coppi et al., 2021). During limestone decomposition, fossil fuel combustion, which is used to provide energy for the process, is an indirect source of CO₂, but this is often accounted for in the energy sector (IPCC, 2021).

The enormous quantity of lime produced in the world (~~~430427.0~~ Mt in 2020; USGS, 2022) is mainly employed in the following sectors (Figure 1): (1) chemical industry, such as for the production of precipitated calcium carbonate (PCC), manufacturing of paper, and refining of sugar; (2) environmental remediation/treatment, including water treatment, acid mine drainage, and flue gas ~~desulphurisation~~~~desulphurization~~; (3) metallurgical industry, for instance as a fluxing agent in the production of iron and steel; and (4) construction industry for building materials including lime mortar and lime-stabilised soil-asphalt mixtures (National Lime Association, 2020). Many lime-based materials, including wastes produced in different industries, re-absorb some of the ~~released CO₂~~~~-released~~, and thereby sequester CO₂ throughout the lime cycle (carbonation), owing to the unstable calcium oxide in these materials (Cizer et al., 2012a). According to Renforth (2019), approximately 34% of lime can directly or indirectly remove CO₂ from the atmosphere and absorb CO₂ during the ~~utilisation~~~~utilization~~ stage. The carbonation process can be described using the following reactions:



Carbonation proceeds progressively from the exterior to the interior of lime-containing materials via the diffusion of CO₂ into particles, followed by its reaction with hydration products of calcium oxide (Cizer et al., 2012b; Despotou et al., 2016). Therefore, carbonation can be considered as a mineralisation technology for carbon capture, ~~utilisation~~~~utilization~~, and storage (CCUS) (Lai et al., 2021; Snæbjörnsdóttir et al., 2020). Samari et al. (2020) indicated that lime-based materials have ~~also~~ been proposed as solid sorbents in direct air capture (DAC) technologies (extraction CO₂ directly from the atmosphere). In practice, however, because of material and environmental factors, only 70–80% of the CaO in lime can be converted into CaCO₃ (Bhatia and Perlmutter, 1983). In previous studies, the carbonation process and factors influencing its rate (Ma et al., 2019), as well as

strategies for improving the sequestration of carbon using lime-containing materials under controlled laboratory conditions (Pan et al., 2012; Baciocchi, 2017), have been examined. Pan et al. (2020), for instance, estimated the CO₂ reduction potential of lime-based solid wastes (e.g., lime mud, red mud and iron and steel slags) in mineralisation technologies, and highlighted a substantial potential for the storage of CO₂ in these wastes. The maximum achievable carbonation capacity of these solid wastes via direct mineralisation is approximately 310 Mt of CO₂ per year. Renforth (2019) estimated the global potential of CO₂ uptake through carbonation of lime and related alkaline materials up to the year 2100 (approximately 2.9–8.5 Gt of CO₂ per year) and indicated that this process can substantially mitigate CO₂ emissions during manufacturing of the associated materials. However, existing studies are limited to estimation of the carbon reduction potential via accelerated carbonation instead of carbon sequestration throughout the lime cycle under realistic conditions.

In the present study, a carbon sequestration analytical model was utilized to evaluate the global uptake of CO₂ by lime-containing materials during the three stages (production, use and waste disposal process) of the lime cycle from 1930 to 2020. The aims were to highlight the magnitude of the lime carbon sink on a global scale and to estimate the net CO₂ emission associated with the production of lime. In addition, characteristics of the uptake of CO₂ by lime and the contribution to the carbon cycle were examined. The present study significantly improves the global carbon uptake model and provides theoretical support for the utilization of lime-containing materials in carbon capture and storage (CCS).

2 Data and Methods

2.1 Lime production, resources usage proportion and treatment

In this study, China and the United States (U.S.) were considered individually, while all other producers were grouped together as “rest of the world” (ROW). The global lime production data came from Lime Statistics and Information (USGS, 2022), but the data did not include the statistics of China's lime production between 1963 and 1984. In addition, the statistical value of China's lime production from 1985 to 2001 was underestimated compared with the actual value (Cao et al., 2019), which led that the statistical data of global lime production during 1963-2001 was significantly less than the actual production (Fig. 2b). The lime production data of China in this study were obtained from (China Construction Material Industry Yearbook, 2022). Considering that lime production data is available for the United States since 1930, which is much earlier than the recorded data for China and the ROW, we filled gaps in the data using fitting methods, thereby extending the time scale of the study to 1930.

First, we fitted China's lime production. The only source of China's lime production statistics is the "China Building Materials Industry Yearbook", which records the lime production data from 1996 to 2020, of which the data from 2015 to 2018 is missing; in addition, the statistical yearbook introduces the use of lime in various industries. From this, we know that the production of lime in construction, steel, calcium carbide, and alumina in the downstream sector of lime accounts for more than 90% of lime production. Therefore, we collected data on China's cement production (1930–2020), the completed area of housing in the whole society (1963–2020), steel production (1949–2020), calcium carbide production (1949–2020), and alumina production

带格式的: 左

批注 [Author1]: This is unclear. Why would the USGS include China? Above you stated that you used the China statistical yearbook for China.

设置了格式: 字体颜色: 红色

(1954–2020) and fitted them to the lime production data. Taking China's lime production as the dependent variable, the stepwise linear regression method was used to construct a regression model. Since the completed area data of houses in the whole society was only available from 1963, the model predicted lime production data from 1963 to 1995. Then, through the ARIMA (0,1,0) model, with external control variables including the steel production, calcium carbide production, and cement production, we fit the lime production in China from 1949 to 1962 (the steel and calcium carbide production data were only extended to 1949). Finally, we used the ARIMA (2,2,0) model without external control variables to fit the lime production in China from 1930 to 1948. From this, we obtained the fitted lime production data for China from 1930 to 2020 (Fig 2a).

After obtaining the Chinese lime production data, we corrected the global lime production data from the USGS from 1930 to 2020 (Fig 2b). The ARIMA (1,0,0) model was then used to fit the global lime production from 1930 to 1962 with global alumina production, steel production and cement production as external control variables.

Relatedly, according to data that were obtained from the USGS, approximately 15%–42% of lime resources in the U.S. are utilized in the chemical industry (mainly for petroleum refining and glass and rubber products production), whereas 30%–51% are employed in metallurgy (primarily in the production of crude steel), 5%–14% are used in the construction industry (principally for the production of lime stabilised soil and lime motor), and approximately 8%–43% are applied in environmental protection and other fields. In the ROW, data on the usage of lime resources in different sectors including the industry were mostly obtained from publications (see the Supplementary Information).

In this study, China and the United States (U.S.) were considered individually, while all other producers were grouped together as “rest of the world” (ROW). The lime production data of China were obtained from China Statistical Yearbook (China Statistical Yearbook, 2022) and the data of U.S. and ROW were from (Lime Statistics and Information | USGS, 2022).

Considering the inconsistent starting year of that the lime production data in (the the United States can be traced back to 1930, but the earliest data in and the lime production data for earlier years in China and the world are not recorded in xx.).

Therefore, we decided to fill in this gap the missing data by using fitting methods, thereby extending the time scale of the study to 1930.

First of all, we adjusted fitted China's lime production. The only statistical source of China's lime production statistics is the "China Building Materials Industry Yearbook", which records the lime production data from 1996 to 2020, of which the data from 2015 to 2018 is missing. In addition, the statistical yearbook also introduces the use of lime in various industries, and more than 90% of lime use. From this, we know that the production of lime in construction, steel, calcium carbide and alumina fields in the downstream sector of lime accounts for more than 90% of lime production, which is the main factors affecting lime production. Therefore, we construct a regression model using stepwise linear regression method, which take China's lime production as the dependent variable, and calcium carbide production, the completed area of houses in the whole society, cement production and alumina production as independent variables. Accordingly, China's cement production (1930–2020), the completed area of housing in the whole society (1930–2020), steel production (1949–2020), calcium carbide production (1949–2020), and alumina production (1954–2020) data to fit the lime production data were collected. we collected China's

130 cement production (1930–2020), the completed area of housing in the whole society (1963–2020), steel production
(1949–2020), calcium carbide production (1949–2020), and alumina production (1954–2020) were fitted to the lime production
data. Taking China's lime production as the dependent variable, the stepwise linear regression method was used to construct a
135 regression model. The independent variables entering the model include calcium carbide production, the completed area of
houses in the whole society, cement production and alumina production. Since the completed area data of houses in the whole
society was only extended to 1963, the model only predicted the lime production data from 1963 to 1995. Then, through the
ARIMA (0,1,0) model, with external control variables including the steel production, calcium carbide production, and cement
140 production, we fit the lime production in China from 1949 to 1962 (the steel and calcium carbide production data were only
extended to 1949). Finally, we use the ARIMA (2,2,0) model without external control variables to fit the lime production in
China from 1930 to 1948. So far, we have obtained the fitted lime production data for China from 1930 to 2020 (Figure 6).
After On the basis of the lime production data obtaining obtained the Chinese lime production in Chinadata, we corrected the
global lime production data from the USGS from 1963 to 2020 (Figure 7). The ARIMA (1,0,0) model was then used to fit the
global lime production from 1930 to 1962 with global alumina production, steel production and cement production as external
145 control variables (Figure 8).

Relatedly, according to data that were obtained from the USGS, approximately 15 %–42 % of lime resources in the U.S. are
utilized in the chemical industry (mainly for petroleum refining and glass and rubber products production), whereas 30 %–
51 % are employed in metallurgy (primarily in the production of crude steel), 5 %–14 % are used in the construction industry
(principally for the production of lime stabilised soil (LSM) and LM), and approximately 8 %–43 % of the resources are
150 applied in environmental protection and other fields. In the ROW, data on the usage of lime resources in different sectors
including the industry were mostly obtained from publications (see the Supplementary Information).

2.2 Estimation of emissions from processes

Regarding industrial processes, lime production is the second-highest source of carbon emissions after cement production, and
thus, its contribution cannot be ignored (Shan et al., 2016a). CO₂ emissions from lime production are mainly linked to the
150 calcination stage, during which calcium oxide (CaO or quicklime) is formed from the decomposition of limestone by heat
(Despotou et al., 2016). Lime comes from the decomposition of limestone in shaft-kiln or rotary kiln, and the carbon emission
of this industrial process is can be estimated from using the IPCC method (IPCC, 2006). Considering the availability of lime
production data, Method 1 (multiplication of the regional lime production by the CO₂ emission factor) from the IPCC
Guidelines for National Greenhouse Gas Inventories was utilised-utilized to calculate CO₂ emissions from lime production
155 processes in the present, and this can be expressed as follows:

$$CE_{l,i} = m_{l,i} \times EF_l \quad (1)$$

设置了格式: 字体颜色: 红色

where $CE_{l,i}$ is the annual CO₂ emissions, $m_{l,i}$ represents the production of the lime industry, and EF_l denotes the CO₂ emission factor associated with the lime production process. l refers to different types of lime use, including PCC, sugar making, lime-stabilized soil and lime mortar, and i refers to different years.

Emission factors for the lime industry processes ~~are were~~ determined using the composition of raw materials and the production technology. In the present study, 0.77-, 0.683-, and 0.75-ton CO₂ per ton of lime produced were adopted as emission factors for the US, China, and ROW, respectively (IPCC, 2006). Emission factors for the U.S. and ROW ~~are were those recommended for developed and developing countries~~ according to the IPCC guidelines, whereas that for China was ~~advanced by from~~ the National Development and Reform Commission of China (~~Guidelines Guidelines Guidelines~~ for provincial greenhouse gas inventories, 2011).

2.3 Assessments of uptake during the lime cycle

Lime materials, which remove CO₂ from the atmosphere, belong to the following stages of the lime cycle: (1) production, (2) ~~utilisation-service~~ and (3) waste disposal (Fig. 1). Therefore, the CO₂ uptake by lime ($C_{l,total}$) was calculated using the following formula:

$$C_{l,total} = C_{l,pro} + C_{l,ser} + C_{l,wd} \quad (2)$$

where $C_{l,pro}$, $C_{l,ser}$, and $C_{l,wd}$ are the uptake components during the production, ~~utilisation-service~~ and waste disposal stages, respectively. The uptake of CO₂ in different stages of the lime cycle is examined subsequently.

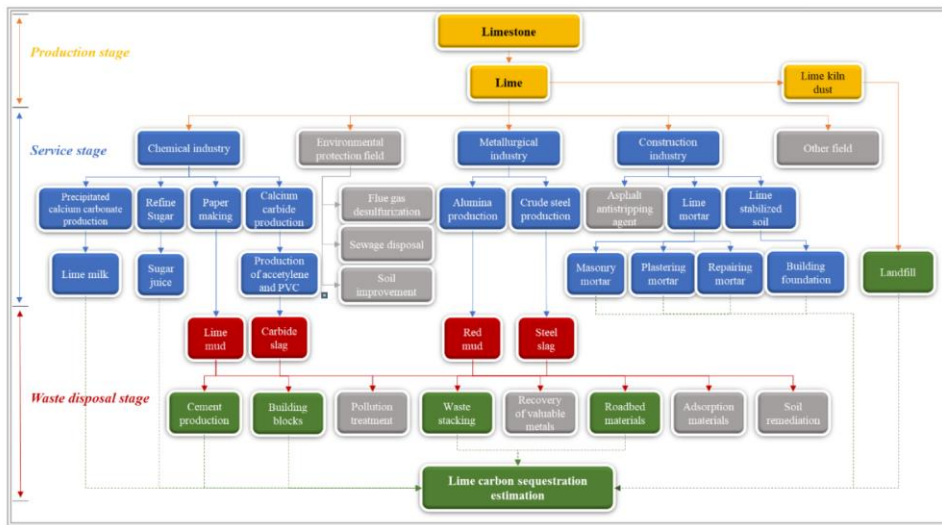


Figure 1: System boundary for the sequestration of carbon by lime. Solid arrows represent the material flow, dashed arrows indicate the carbon flow, and double solid lines represent accounting boundaries.

175 2.3.1 Assessment of uptake during the production stage

The carbon sink of the lime production stage refers to the uptake of CO₂ by lime kiln ash, and this can be quantified using the following expression:

$$C_{l,pro} = m_{l,i} \times r_{lkd} \times f_{lkd}^{CaO} \times \gamma_{lkd} \times \frac{M_{CaO}C}{M_{CaO}} \quad (3)$$

where $m_{l,i}$ is the quantity of lime produced, r_{lkd} represents the output rate of lime kiln ash, f_{lkd}^{CaO} denotes the concentration of CaO in dust, γ_{lkd} is the rate of conversion of CaO to CaCO₃ in dust, and M_{CaO} and M_{CO_2} are molar masses of CaO and CO₂, which in the present study are 56 and 44.01 g/mol, respectively.

2.3.2 Assessment of uptake during the service stage

Processes that can absorb CO₂ in the lime utilisation-utilization stage principally comprise the production of **Precipitated precipitated** calcium carbonate (PCC, $C_{pcc,i}$), carbonation sugar (SUG, $C_{sug,i}$), lime-stabilised soil (LSS, $C_{lss,i}$), and lime mortar (MOR, $C_{mor,i}$). The uptake of CO₂ in this stage can be calculated as follows:

$$C_{l,ser} = C_{pcc,i} + C_{sug,i} + C_{lss,i} + C_{mor,i} \quad (4)$$

185 (1) **Precipitated calcium carbonate**CC and **carbonation sugars**SUG

PCC is produced via the hydration of high-calcium quicklime, followed by a reaction of the resulting slurry and CO₂ (Wang *et al.*, 2002), and this reaction can be represented as follows: Ca(OH)₂+CO₂=CaCO₃↓+H₂O. According to the law of conservation of mass, the uptake of CO₂ by lime in PCC can be calculated as follows:

$$C_{pcc,i} = m_{l,i} \times L_1 \times a_1 \times f_l^{CaO} \times \frac{M_{CO_2}C}{M_{CaO}} \quad (5)$$

where L_1 is the proportion of lime that is used in the chemical industry, a_1 is the proportion of lime utilized in the chemical industry that is associated with PCC, and f_l^{CaO} is the concentration of CaO in lime. Similar to the principle of the carbon sink in the production of PCC, the uptake of CO₂ linked to the production of carbonation sugars (SUG) can be calculated using the following expression:

$$C_{sug,i} = m_{l,i} \times L_1 \times a_2 \times f_{sug} \times f_l^{CaO} \times \frac{M_{CO_2}C}{M_{CaO}} \quad (6)$$

where a_2 is the proportion of lime used in the production of SUG in the industry and f_{sug} is the proportion of sugar produced using the lime-refining method.

195 (2) **Lime stabilised soil**LSS

Under wet conditions, the carbonation rate of a LSS is approximately between 70-%-80-% over a duration of three months (Liu et al., 2018b). Therefore, it is assumed that LSS can be carbonated within a year, and the uptake of CO₂ by LSS is quantified using the following expression:

$$C_{lss,i} = m_{l,i} \times L_2 \times a_3 \times f_l^{CaO} \times \gamma_{lss} \times \frac{M_{CaO-C}}{M_{CaO}} \quad (7)$$

where L_2 is the proportion of lime used in the construction sector, a_3 represents the proportion of lime employed in LSS in the construction sector, and γ_{lss} is the rate of conversion of CaO to CaCO₃ in LSS.

(3) Lime mortar MOR

MOR is mostly used for the plastering of interior walls, with a typical thickness of 20 mm (Almanac of China building materials industry, 2022). Under natural conditions, the estimated carbonation rate of MOR is 1 mm d^{-0.5} (Ventol et al., 2011). Therefore, according to Fick's law of diffusion, a year is insufficient for the complete carbonation of a MOR layer. Consequently, the uptake of CO₂ by MOR is calculated using the following expressions:

$$C_{mor,i} = m_{l,i} \times L_2 \times a_4 \times f_{mor,i}^{CaO} \times \gamma_{mor} \times \frac{M_{CaO-C}}{M_{CaO}} \quad (8)$$

$$d_{mor} = k_{mor} \times \sqrt{t_{mor}} \quad (9)$$

$$f_{mor,i} = (d_{mor,i} - d_{mor,i-1}) / d_T \quad (10)$$

where L_2 is the proportion of lime used in the construction sector, a_4 denotes the proportion of lime in MOR that is utilized in the construction sector, $f_{mor,i}$ represents the carbonation ratio of MOR in the i -th year, γ_{mor} is the rate of conversion of CaO to CaCO₃ in MOR, $d_{mor,i}$ represents the depth of carbonation of MOR in the i -th year; k_{mor} denotes the rate of carbonation of MOR, t_{mor} is the duration of carbonation of MOR and d_T is the thickness of MOR.

2.3.3 Assessment of uptake during the waste disposal stage

Lime employed in the production of paper, aluminium, calcium carbide, and steel generates by-products including lime mud (LM, $C_{LM,i}$), red mud (RM, $C_{RM,i}$), carbide slag (CS, $C_{CS,i}$), and steel slag (SS, $C_{SS,i}$), respectively. The alkaline component (CaO) in these wastes absorb CO₂ under natural conditions.

(1) Lime and red mud LMs and RM

Lime mud particles that are involved in the production of paper are usually fine and evenly distributed (Ma et al., 2021). In fact, particles < 40 μm account for 93-%, and the associated water contents range from 39-% to 60-% (Qin et al., 2015). However, as a paste, the penetration of CO₂ to react with the lime mud is limited. Consequently, a year is usually insufficient for the complete carbonation of lime mud.

Red mud is also characterised by fine particles as well as a porous structure, high specific surface area, and good stability in water (Wang et al., 2019). Similar to the principle of the carbon sink for lime mud, a year is insufficient for the complete

carbonation of red mud (Liu et al., 2018b). The uptake of CO₂ by lime in lime and red muds is calculated using the following expression:

$$\varepsilon_{m,ij} = m_{p,ij} \times r_{m,ij} \times f_{m,j}^{CaO} \quad (11)$$

where $\varepsilon_{m,ij}$ denotes the mass of CaO in wastes (m_j=lime mud or red mud) that can be carbonated in year i, $m_{p,ij}$ is the quantity of paper and paperboard/alumina that are produced in the i-th year, and p is the production, where $c_{m,ij}$ denotes the mass of CaO in wastes (j=lime mud or red mud) that can be carbonated in year i, $m_{p,ij}$ is the quantity of paper and paperboard/alumina that are produced in the i-th year, $r_{m,ij}$ is the output rate of waste j and $f_{m,j}^{CaO}$ represents the concentration of CaO in waste j.

According to Fick's law of diffusion, the depth of carbonation of waste j ($d_{m,ij}$) can be obtained from the carbonation rate ($k_{m,j}$) and carbonation time (t_i) using the following expressions/equations:

$$d_{m,ij} = k_{m,j} \times (\sqrt{t_i} - \sqrt{t_{i-1}}) \quad (12)$$

$$R_{m,ij} = \begin{cases} \frac{k_{m,j} \times \sqrt{t_i}}{h_{m,j}} \times t_i & (t_i \leq t_{m,j}) \\ \frac{d_{m,ij}}{h_{m,j}} & (t_{m,j} < t_i < 100) \end{cases} \quad (13)$$

where $R_{m,ij}$ represents the fraction of waste j that is carbonated in the i-th year, $h_{m,j}$ is the height of the waste j pile and $t_{m,j}$ is the duration of the yard of the waste j. Accordingly,

$$C_{m,ij} = \varepsilon_{m,ij} \times (1 - f_{m,ij}^{use}) \times R_{m,ij} \times \gamma_{m,j} \times \frac{M_{CaO} C}{M_{CaO}} \quad (14)$$

where $C_{m,ij}$ is the uptake of CO₂ uptake of waste j during the i-th year, $f_{m,ij}^{use}$ denotes the utilisation/utilization rate of waste j and $\gamma_{m,j}$ is the rate of conversion of CaO to CaCO₃ in lime mud.

(2) Carbide-slagS

Carbide slag comprises particles that are dominantly between 10–50 μm, which usually contain moderate amounts of water (Lin et al., 2006). Stacking for approximately 15 d can reduce the concentration of CaO by approximately 50% (Hao et al., 2013). The uptake of CO₂ by CS can be calculated using the following expressions:

$$\varepsilon_{cs,i} = m_{l,i} \times L_1 \times a_5 \times p_i^{cs} \times r_{cs} \times f_{cs}^{CaO} \quad (15)$$

$$C_{cs,i} = \varepsilon_{cs,i} \times (1 - f_{cs}^{use}) \times \gamma_{cs} \times \frac{M_{CaO} C}{M_{CaO}} \quad (16)$$

where $\varepsilon_{cs,i}$ is the mass of CaO in CS in the i-th year, a_5 denotes the proportion of lime in calcium carbide that is utilized in the chemical industry, p_i^{cs} represents the output of calcium carbide per ton of lime input, r_{cs} is the output rate of CS, f_{cs}^{CaO} is the concentration of CaO in CS, f_{cs}^{use} is the utilisation/utilization rate of CS and γ_{cs} is the rate of conversion CaO to CaCO₃ in CS.

(3) Steel-slagS

格式化表格

Steel-slagS cannot be carbonated within a year because its hydration commonly requires more than 4 years (Wang and Yan, 2010). In the present study, the SS particle was approximated as a uniformly-densified sphere. The fraction ($R_{s,i}$) of SS that is carbonated can be estimated using the following expressions (Xi et al., 2016):

$$D_{ss,i} = 2d_{ss,i} = 2k_{ss} \times \sqrt{t_i} \quad (17)$$

$$R_{s,i} = \begin{cases} 100\% - \int_a^{D_{ss,i}} \frac{\pi}{6} (D - D_{ss,i})^3 / \int_a^b \frac{\pi}{6} D^3 \times 100\% & (a > D_{ss,i}) \\ 100\% - \int_{D_0}^{D_{ss,i}} \frac{\pi}{6} (D - D_{ss,i})^3 / \int_a^b \frac{\pi}{6} D^3 \times 100\% & (a \leq D_{ss,i} \leq b) \\ 100\% & (b < D_{ss,i}) \end{cases} \quad (18)$$

$$\Delta R_{s,i} = R_{s,i} - R_{s,i-1} \quad (19)$$

where $D_{ss,i}$ is the maximum diameter of SS that complete carbonation in the i -th year, $d_{ss,i}$ represents the depth of carbonation of SS in the i -th year, k_{ss} is the rate of carbonation of SS, t_i is the carbonation duration, D is the diameter of SS, a and b are the minimum and maximum SS diameters, respectively, and a and b represent the corresponding minimum and maximum diameters of SS particles in a given size distribution. The annual carbonation of SS ($C_{ss,i}$) can then be calculated

using the following expressions:

$$\varepsilon_{ss,i} = m_{s,i} \times r_{ss} \times f_{ss}^{CaO} \quad (20)$$

$$C_{ss,i} = \varepsilon_{ss,i} \times \Delta R_{s,i} \times f_{ss}^{use} \times \gamma_{ss} \times \frac{M_{CaO}}{M_{CaCO_3}} \quad (21)$$

where $\varepsilon_{ss,i}$ is the mass of CaO in SS in the i -th year, $m_{s,i}$ represents the mass of crude steel that was produced in the i -th year, r_{ss} is the output rate of steel-slagSS, f_{ss}^{CaO} is the concentration of CaO content in steel-slagSS, f_{ss}^{use} is the ratio of SS that is utilized as stacking and roadbed material and γ_{ss} is the rate of conversion of CaO to CaCO₃ in SS.

2.4 Calculation of annual and cumulative uptakes

Even though the uptake of carbon can be estimated using alkaline materials in different stages of the lime cycle, the global and regional CO₂ absorption values were obtained via the aggregation of all alkaline materials. In the global and regional carbon sink accounting, parameters such as the production of lime, proportion of lime utilized in different sectors, diffusion or carbonation coefficient, output rate, concentration of CaO, conversion ratio of CaO to CaCO₃, and particle size distribution and height of lime or red mud pile among others, were utilized as inputs for the model (see the Supplementary Information).

Basically, for the uptake of CO₂ in year t_i , the cumulative uptake of CO₂ in year t_i minus that for year t_{i-1} can be obtained from the following expression:

$$\Delta C_{l,total}^{t_i} = \sum C_{l,total}^{t_i} - \sum C_{l,total}^{t_{i-1}} \quad (22)$$

and thus, the contribution of the annual uptake of carbon to the total carbonation can also be calculated.

2.5 Uncertainty analysis

We identified 16 groups of impact factors associated with the estimation of lime process carbon emission and carbon sequestration estimations, which included disaggregated 115 input-specific parameters, each with a specific statistical distribution (see the Supplementary Information). ~~Because of~~Due to the difficulties in obtaining the true values of the parameters, we employed the Monte Carlo approach recommended by the 2006 IPCC Guidelines for National Greenhouse Gas Inventories; to evaluate assess access the uncertainties for the carbon emission and removal of lime materials. We fed the statistical characteristics of the 115 variables into our models, and the simulated carbon emission and removal results were obtained through a 100,000 Monte Carlo iteration 100,000 iteration Monte Carlo iterations simulation. Subsequently, ~~Subsequently, the s~~statistical analysis was then performed ~~conducted~~ to derive the median and the corresponding lower and upper bounds of the 95% confidence intervals (CI) for the carbon uptake and emission of lime materials.

A Monte Carlo analysis was used to determine the uncertainty associated with the uptake of carbon by lime. This uncertainty originates from input parameters (e.g. activity level data and carbon absorption factors) of the carbon sink accounting for model and quality of the statistics infrastructure. In the present study, 53 causes of uncertainty (see the Supplementary Information) associated with the estimated uptake of CO₂ were identified after more than 100,000 simulations.

3 Results

3.1 Aggregated regional and global emissions from the production of lime

The lime yield of various countries is shown in Figure 2a. ~~To compensate for the underestimation of carbon sink and carbon emissions caused by the lack of data as much as possible (Cao et al., 2019), different data interpolation methods and parameters (as mentioned in the Section 2.1) were adopted to fit the lime output for 1930–1948, 1949–1962, and 1963–1995. The different interpolation methods and parameters led to changes in the uncertainty range, as shown in Figure 2a, which was reflected in the sudden change of data in the node years of piecewise fitting (such as 1948, 1949, 1963).~~

Considering the shortcomings of the global lime output statistics, this paper has made corresponding corrections to the global lime output data based on China's lime output data (Fig. 2b). From 1930 to 2001, the cumulative value of compensated global lime production in this study is 7023.30 Mt from the missing data of China. Since 2001, the lime production in this study is a slightly lower than that of USGS, due to the different reference sources of Chinese data. In general, the global lime output fluctuated and increased over time, from 139.62 Mt in 1930 to 394.93 Mt in 2019. In the early 1930s, the lime output decreased slightly, which may be due to the impact of the 'The Great Depression' and the closure of many factories, resulting in a decrease in the global lime output. In 2020, affected by the COVID-19, the lime production dropped slightly to 391.64 Mt (USGS: 427 Mt).

Figure 2c shows the estimated CO₂ emissions from lime production processes in China, the U.S., ROW and at a global scale

设置了格式: 字体颜色: 红色

设置了格式: 字体颜色: 红色

设置了格式: 字体颜色: 红色

设置了格式: 字体颜色: 红色

设置了格式: 字体颜色: 红色

设置了格式: 字体颜色: 红色

设置了格式: 字体颜色: 红色

设置了格式: 字体颜色: 红色

设置了格式: 字体颜色: 红色

设置了格式: 字体颜色: 红色

设置了格式: 字体颜色: 红色

设置了格式: 字体颜色: 红色

设置了格式: 字体颜色: 红色

设置了格式: 字体颜色: 红色

设置了格式: 字体颜色: 红色

设置了格式: 字体颜色: 红色

设置了格式: 字体颜色: 红色

设置了格式: 非突出显示

设置了格式: 非突出显示

设置了格式: 非突出显示

设置了格式: 非突出显示

设置了格式: 非突出显示

设置了格式: 非突出显示

批注 [T2]:

设置了格式: 字体: (默认) Times New Roman, 10 磅, 字体颜色: 红色, 图案: 清除

设置了格式: 字体: (默认) Times New Roman, (中文) Times New Roman

from 1930 to 2020. According to our calculations, the global process CO₂ emissions increased from with 27.39 Mt C yr⁻¹ (95% Confident Interval, CI: 8.87–46.86 Mt C) in 1930 to 75.73 Mt C yr⁻¹ (95% CI: 69.18–82.33 Mt C) in 2020. In the early 1930s, carbon emissions slightly declined due to the impact of lime production and its uncertainty. The uncertainty of lime output can be transferred to the final simulation results of lime carbon emissions. The greater uncertainty of the parameters will lead to greater uncertainty in the simulation results. The results of the 10,000 iteration Monte Carlo simulation show the change trend (Figure 2c). On a global scale, emissions doubled from 44.63 Mt C yr⁻¹ in 2002 to 75.73 Mt C yr⁻¹ in 2020. During this period (2002–2018), the average annual rate of increase was 2.98%, which was significantly higher than the rate for 1930–2002 (0.68%). The cumulative emissions of CO₂ from 1930 to 2020 were 3720.16 Mt C (95% CI: 3166.18–4287.43 Mt C). Emissions decreased in 2009, which was likely caused by the global financial crisis in 2008, during which downstream lime industries experienced severe problems, such as excess produce, low production quantities, and stiff competition (Dong et al., 2010).

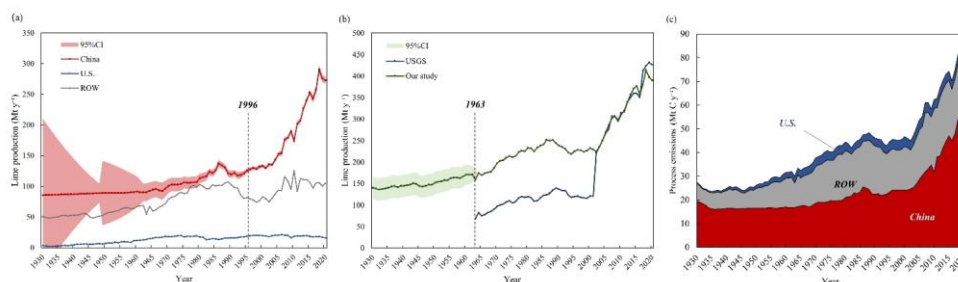


Figure 2: (a) Lime production in different countries or regions from 1930 to 2020. Shadows represent uncertainty ranges. CI: Confidence interval. (b) Global lime production from 1930 to 2020. (c) Annual CO₂ emissions from industrial processes.

CO₂ emissions from 1930 to 2020 in China account for approximately half of the global total. China was primarily responsible for the increase in the global emission from lime production processes during the studied period. In China, from 1930 to 2020, the average annual lime process CO₂ emission was 23.08 Mt C yr⁻¹, with 1.06% average annual growth rate. Notably, a rapid global increase in CO₂ emissions started in 2002. From 2002 to 2020, the average annual growth rate of carbon emissions from lime was 4.03%, which was far higher than that of 1930 to 2001 (0.32%). This was mainly due to the steady growth of China's macro economy after 2002. This finding was consistent with estimates from studies on the uptake of carbon by cement carbon based on similar approaches (Cui et al., 2019). These results are closely linked to the development of downstream sectors of the lime industry in China, such as the iron and steel, light and chemical, construction and materials industries (Shan et al., 2016b). In 2020, CO₂ emissions in China from lime production processes reached 49.93 Mt C yr⁻¹ (95% CI: 44.18–55.94 Mt C), and the cumulative emission was 2100.39 Mt C (95% CI: 1606.96–2620.93 Mt), accounting for 56.33% of the global total. This figure is higher than the 46.91 Mt C yr⁻¹ forecasted for 2020 by Tong et al. (2019), which can be attributed mainly to the emission reduction scenarios considered.

320 In the U.S., from 1930 to 2020, CO₂ emissions from lime production processes remained at around 2.72 Mt C yr⁻¹, and the cumulative emissions by 2020 were approximately 247.30 Mt C, which represents 6.63% of the global total. This relatively low value is because of a fairly stable production of lime in the U.S. and significant import of lime from Canada (USGS, 2022). Relatedly, for the ROW, the cumulative emission was 1380.77 Mt C, which represents 37.03% of the global total.

325 ~~Th withoutal data and the small China's lime production estimation during 1985-1995 (Cao et al., 2019) induced the significant lower compensate as much as possible the missing result in the the the.~~ Considering shortcomings lime rease lime production Figure 2 shows the estimated CO₂ emissions from lime production processes in China, the U.S., ROW and at a global scale from 1963 to 2020. Globally (Fig. 2a), ~~with, CI~~ lime emissions of CO₂ from lime production processes doubled from 0.15 Gt yr⁻¹ (95% Confident Interval: 0.14-0.17 Gt) in 2002 to 0.30 Gt yr⁻¹ (95% CI: 0.27-0.32 Gt) in 2020. During this period (2002-2020), the average annual rate of increase was 3.41%, which is significantly higher than the rate for 1963-2002 (0.73%). The cumulative emissions of CO₂ from 1963 to 2020 is 10.17 Gt (95% CI: 9.06-11.32 Gt), but emissions decreased in 2009. This decrease was likely caused by the global financial crisis in 2008, during which downstream lime industries experienced severe problems, such as excess produce, low production quantities, and stiff competition (Dong et al., 2010). The trend of global net lime emissions is basically similar to that of emissions, with a cumulative net emission of 9.06 Gt from 1963 to 2020.

335 Changes in emissions of CO₂ from 1963 to 2020 in China are displayed in Fig. 2b, and these accounts for approximately 50% of the global emission. Alternatively, China was primarily responsible for the increase in the global emission from lime production processes during the studied period studied. In China, from 1963 to 2020, the average annual lime process CO₂ emission of CO₂ was 98 Mt yr⁻¹, and with 1.03% the average annual growth rate of increase was 2.13%. Notably, the rapid global increase in CO₂ emissions started in 2002. From 2002 to 2020, the average annual growth rate of carbon emissions from lime is 4.86%, which is 7.5 times that of 1963 to 2001. This is mainly due to the steady growth of China's macro economy after 2002. This finding is consistent with estimates from studies on the uptake of carbon by cement carbon-based on similar approaches (Cui et al., 2019). These results are closely linked to the development of downstream sectors of the lime industry in China, such as the iron and steel, light and chemical, construction and materials industries (Shan et al., 2016b). By In 2020, lime process CO₂ emissions of CO₂ in China attained reached to 211 Mt yr⁻¹ (95% CI: 187-236 Mt), whereas while the cumulative emission was 5700 Mt (95% CI: 4849-6628 Mt), and this accounted ing for 56.03% of the global CO₂ emissions associated with lime production processes. The result that was obtained in the present study is higher than the 172 Mt yr⁻¹ that was forecasted for the same period by Tong et al. (2019), and this difference is attributed mainly to the emission reduction scenarios that are considered in each study.

340 In the U.S., from 1963 to 2020, CO₂ emissions from lime production processes remained at around 12 Mt yr⁻¹, and the cumulative emissions by 2020 were approximately 753 Mt, and this represents 13.21% of the global emission. This relatively low value is because of a fairly stable production of lime in the U.S. and significant import of lime from Canada (Lime Statistics and Information | U.S. Geological Survey, 2022). Relatedly, for the ROW, the cumulative emission was 71 Mt, and this represents 24.4% of the global emission.

设置了格式: 字体颜色: 红色

3.2 Lime uptake of carbon by regions

355 According to the lime carbon sequestration model, utilized in the present study to estimate the annual carbon in sinks in
different regions, the global uptake of CO₂ by lime-containing materials increased from 38.259.16 MtMt C (95-% CI:27.85-
51.381.84-18.76 MtMt C) in 19631930 to 134.3334.84 MtMt C (95-% CI:90.3723.50-193.2949.81 MtMt C) in 2020,
representing and this represents an average annual growth rate of increase of 2.291.50% (Fig 3a). Figure 3b shows the annual
360 uptake of CO₂ in different regions, where the area represents the cumulative uptake in each region under natural
conditions. Figure 3 shows the annual uptake of CO₂ in different regions and stages of the lime cycle between 1963 and 2020,
whereas the area represents the cumulative uptake in each region under natural conditions. In the early 1930s, the carbon sink
of lime was affected by the uncertainty of lime production parameters, and the trend was slightly decreased, which was similar
to the change of carbon emissions in lime industrial process. Cumulatively, 1444.70 Mt C (95% CI:1016.24-1961.05 Mt C)
365 were sequestered by lime-containing materials between 1930 and 2020. This means that 38.83% of CO₂ emissions from the
production process of calcining limestone process were offset by lime carbon uptake at the same stage (1930-2020).
Cumulatively, 4053.61 Mt of CO₂ (95-% CI:3016.63-5251.90 Mt) were sequestered by lime-containing materials between
1963 and 2020. The highest sequestration was in China (-63.123.95-%, 2542.94918.41 MtMt C) because of the associated
high production of lime materials (China Statistical Yearbook, 2022), followed by the ROW (-33.7134.35-%, 1358.23474.35
MtMt C) and the US (-3.16-01-%, 127.4143.28 MtMt C). China's lime carbon sink is greatly affected by lime production, so
370 its change is actually similar to that of lime production. The change of China's lime carbon sink was not obvious before the
20th century, fluctuating at 7.95 Mt C yr⁻¹. Until 2002, the total amount of carbon sink increased year by year with the increase
of lime production. As seen in Fig. 3a, in China, lime carbon uptake increased from 10.52 Mt C in 2002 to 24.46 Mt C in 2020.
Taking into account the data from 1930 to 2001 that we have fitted, we have compensated for the underestimation of China's
lime carbon sink (cumulative 467.85 Mt C). Affected by the COVID-19, the amount of China's lime carbon sink decreased in
375 2020 compared with that in 2019 (about 24.94 Mt C). For other regions, lime carbon sinks in the United States (from 0.08 Mt
C in 1930 to 0.66 Mt C in 2020) and the ROW (from 1.49 Mt C in 1930 to 9.24 Mt C in 2020) showed an overall trend of
increasing over time.

设置了格式: 突出显示

设置了格式: 上标

设置了格式: 英语(英国)

设置了格式: 字体: (默认) Times New Roman, (中文) Times New Roman, 英语(英国)

设置了格式: 英语(英国)

设置了格式: 字体颜色: 红色

设置了格式: 字体颜色: 红色

设置了格式: 字体颜色: 红色

设置了格式: 字体颜色: 红色

设置了格式: 字体颜色: 红色

设置了格式: 字体颜色: 红色

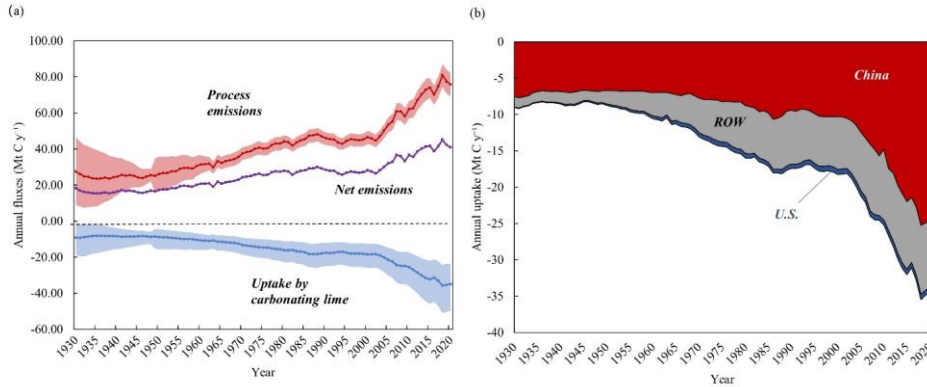
设置了格式: 字体: (默认) Times New Roman, 10 磅, 字体颜色: 自动设置, 图案: 清除

设置了格式: 字体: (默认) Times New Roman, 10 磅, 字体颜色: 自动设置, 图案: 清除

设置了格式: 字体: (默认) Times New Roman, 10 磅, 字体颜色: 自动设置, 图案: 清除

设置了格式: 字体: (默认) Times New Roman, 10 磅, 字体颜色: 自动设置, 图案: 清除

Obviously, variation trends in the three regions from 1963 to 2020 are similar (see the Supplementary Information).



380 **Figure 3: (a) Net lime emissions from 1930 to 2020. Shadows represent uncertainty ranges, (b) Annual uptake of carbon dioxide by lime in different regions, ROW: Rest of World.**

The cumulative uptakes of CO₂ by lime materials in different regions are displayed in Fig. 44. Notably, the top three lime-containing materials (LSS, MOR and SS) accounted for 81.82-73.75% of the global-total global CO₂ uptake by lime uptake of CO₂ by such materials. Regarding China, the cumulative uptake of CO₂ by all lime materials was 2542.94918.41 MtMt C, and the amount of CO₂ that was removed by LSS-LSS (-1360.96487.15 MtMt C) exceeds-exceeded the sum removed by all other materials (Fig. 4a). In the U.S., the uptake was dominated by carbonating SS (Fig. 4b), LSS, and SUG-. The cumulative carbon sink of these three materials and the cumulative amounts were 42.6414.80, 22.577.26 and 21.066.69 MtMt C, respectively. In the ROW, SS (558.97175.72 MtMt C), LSS (369.23125.05 MtMt C), and MOR (488.3761.67 MtMt C) constituted-were the top three materials (Fig. 4e).

- 设置了格式: 字体颜色: 红色
- 设置了格式: 字体: (中文)+中文正文(等线), (中文)中文(简体, 中国大陆)
- 设置了格式: 字体: (默认) Times New Roman, 小五, 字体颜色: 红色, 英语(英国)
- 设置了格式: 字体: (默认) Times New Roman, 小五, 字体颜色: 红色, 英语(英国)
- 设置了格式: 字体: (中文)+中文正文(等线), 字体颜色: 红色, (中文)中文(简体, 中国大陆)
- 设置了格式: 字体: (默认) Times New Roman, 小五, 字体颜色: 红色, 英语(英国)
- 设置了格式: 字体: (中文)+中文正文(等线), (中文)中文(简体, 中国大陆)
- 设置了格式: 字体: (中文)+中文正文(等线), 字体颜色: 红色, (中文)中文(简体, 中国大陆)
- 设置了格式: 字体颜色: 红色
- 设置了格式: 字体: (中文)+中文正文(等线), 字体颜色: 红色, (中文)中文(简体, 中国大陆)

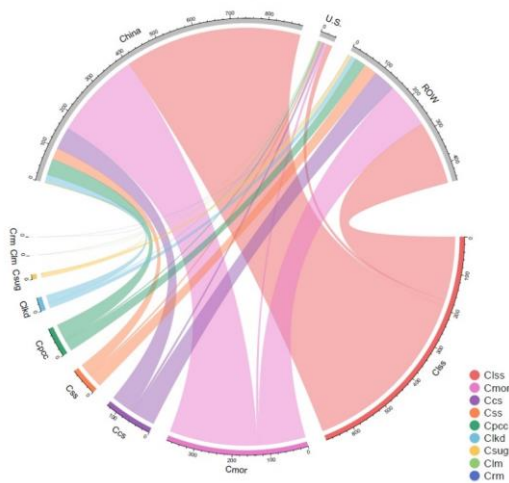


Figure 4: Cumulative uptake of CO₂ uptake by lime-containing materials in different regions. ROW: Rest of World, Ccs: CO₂ uptake by carbide slag, Clkd: CO₂ uptake by lime kiln dust, Clss: CO₂ uptake by lime-stabilised soil, Cmor: CO₂ uptake by lime mortar, Cpcc: CO₂ uptake by Precipitated calcium carbonate, Crm: CO₂ uptake by red mud, Ccs: CO₂ uptake by steel slag, Csug: CO₂ uptake by carbonation sugar, Clm: CO₂ uptake by lime mud.

设置了格式: 字体颜色: 红色

设置了格式: 字体颜色: 红色, 下标

设置了格式: 字体颜色: 红色

3.3 Uptake of CO₂ in different stages of the lime cycle

Among the stages of the lime cycle, the utilisation-service stage accounted for the highest uptake of CO₂ (2922.661076.97 MtMt C) from 19631930 to 2020, and this representsing 74.0576.21-%% of the total. Relatedly, the uptake of CO₂ during the production and waste disposal stages were 101.6636.95 and 933.64299.19 MtMt C, respectively (Fig. 2b5).

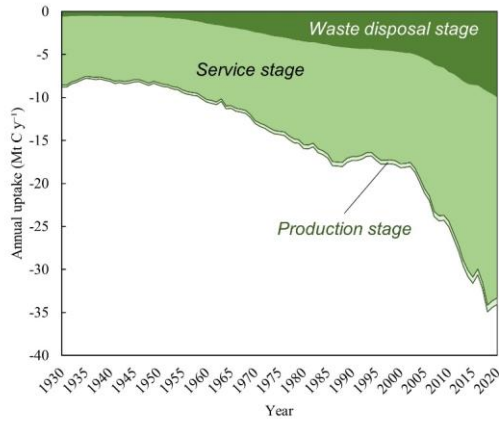


Figure 5: Global annual uptake of carbon dioxide by lime in different stages of its cycle.

Since 1963, the production stage is associated with a significant amount-output of lime kiln dust (LKD) dust, which is a by-product of the production of lime. The uptake of CO₂ by this dust in 2020 attained was 2.950.74 MtMt C. This contribution is attributed to the development of the lime industry and the increase in the disposal of lime kiln dust (LKD) in landfills (Latif et al., 2015). The concentration of CaO in the ash of lime kilns is approximately 54.88%, and thus, this continuously absorbs CO₂ in landfills (Bobicki et al., 2012).

The annual and cumulative uptake of carbon by lime materials during the utilisation-service stage varied significantly, but these produced the following trend: LSS > MOR > PCC > SUG (Table 1). As commonly used building materials, LSS and MOR correspondingly removed 4729.04629.43 and 837.77316.89 Mt of CO₂. Considering the consumption of lime in the construction sector over the past five decades and its increasing utilisation-utilization worldwide, especially in China and other developing countries, its uptake of CO₂ will certainly increase in the future (Renforth, 2019). The carbon fixation amounts of PCC and SUG of 233.3084.98 and 125.5445.68 MtMt C, respectively, accounted-accounting for <<10-% of the total uptake during the utilisation-utilization stage.

Table 1. Summary of the global uptake of CO₂ by lime-containing materials in different stages of its cycle

Stage	Types of lime materials	CO ₂ uptake in 2020 (Mt C)	Cumulative CO ₂ uptake from 1930 to 2020 (Mt C)
Production	LKD	0.76	36.95
Service	LSS	13.96	629.43
	MOR	6.88	316.89

设置了格式: 字体颜色: 红色

设置了格式: 字体颜色: 红色

设置了格式: 字体颜色: 红色

带格式的: 左, 缩进: 左侧: 0.35 厘米, 首行缩进: 0 厘米, 右侧: 0.35 厘米

带格式的: 缩进: 首行缩进: 0 厘米

设置了格式: 字体: (默认) Times New Roman, (中文) Times New Roman

格式化表格

设置了格式: 字体颜色: 红色

设置了格式: 字体颜色: 红色

设置了格式: 字体颜色: 红色

设置了格式: 字体颜色: 红色

设置了格式: 字体颜色: 红色

设置了格式: 字体颜色: 红色

Stage	Types of lime materials	CO ₂ uptake in 2020 (Mt C)	Cumulative CO ₂ uptake from 1930 to 2020 (Mt C)
Waste disposal	PCC	1.73	84.98
	SUG	0.74	45.68
	RM	0.002	0.05
	SS	8.31	225.67
	CS	1.67	73.39
	LM	0.003	0.09

LKD: Lime Kiln Dust, LSS: Lime-Stabilized Soil, PCC: Precipitated Calcium Carbonate, SUG: Carbonation Sugar, RM: Red Mud, SS: Steel Slag, CS: Carbide Slag, LM: Lime Mud.

420 Regarding the waste disposal stage, ~~the~~ CO₂ absorption ~~is~~ was mainly associated with carbonation of SS (Table 1). The cumulative uptake estimated d in the present study ~~is~~ was 721.33225.67 MtMt C. The iron and steel industry, which is a basic industry in industrialised countries, produces approximately 180–270 Mt of SS annually (Iron and Steel Slag, 2022). However, the alkaline content of SS is due to the high amount of lime used in the iron and steel making process. Therefore, SS sequesters a high amount of CO₂ in stockpiles and as roadbed material (Bobicki et al., 2012). Owing to its elevated concentration of Ca(OH)₂, high specific surface area and efficient carbonation process, CS is linked to the sequestration of approximately 200.8473.39 MtMt C-of CO₂ (Huang et al., 2004; Hao et al., 2013). The total uptake of ~~red-RM~~ and ~~lime-muds~~ LM is approximately 0.45-0.14 Mt-of CO₂ (Table 1). This low uptake is assigned to the high content of water in these wastes, which hinders the diffusion of CO₂ into their particles under exposure.

4. Discussion

430 Although the national greenhouse gas inventories guideline involves methods for quantifying CO₂ emissions that are linked to lime production processes, ~~carbon sequestration of lime was not considered in the IPCC neglected-carbon-sequestration-by-lime~~ (IPCC, 2006). According to the analysis conducted in the present study, the uptake by lime-containing materials rapidly increased from ~~1963~~ 1930 to 2020 in all stages of the lime cycle. In 2020, the global uptake of CO₂ by lime was equivalent to 2.15% of the global industrial emissions of CO₂; therefore, neglecting this sink caused an overestimation of the global carbon emission from industrial processes. Regarding the global carbon cycle, the annual carbon uptake by lime was approximately 1.65% of the average global forest ecosystem sink from 2001 to 2010, and this can explain approximately 1.55% of the missing global carbon sink (2.37 Gt C yr⁻¹) (Data supplement to the Global Carbon Budget 2021, 2022). Therefore, if the lime sink is incorporated, the global carbon budget, which already includes data for carbon sinks of the ocean, land, and cement can be improved.

440 Table 2. Comparison of CO₂ uptake by different types of materials

格式化表格

设置了格式: 字体颜色: 红色

设置了格式: 字体颜色: 红色

设置了格式: 字体颜色: 红色

设置了格式: 字体颜色: 红色

设置了格式: 字体颜色: 红色

设置了格式: 字体颜色: 红色

设置了格式: 字体颜色: 红色

设置了格式: 字体颜色: 红色

设置了格式: 字体颜色: 红色

设置了格式: 字体颜色: 红色

设置了格式: 字体颜色: 红色

设置了格式: 字体颜色: 红色

带了格式: 缩进: 左侧: 0 厘米

带了格式: 缩进: 首行缩进: 0 厘米

设置了格式: 字体颜色: 红色

设置了格式: 字体颜色: 红色

设置了格式: 字体颜色: 红色

设置了格式: 字体颜色: 红色

设置了格式: 字体颜色: 红色

设置了格式: 字体颜色: 红色

设置了格式: 字体颜色: 红色

Region	Carbon sink type	Annual CO ₂ uptake (Mt C yr ⁻¹)	Source
Global	Carbonate	660–1120	(Li et al., 2018)
Global	Silicate	34.64	(Zhang et al., 2021)
Global	Lime	23.50–49.81	this study
Global	Cement	207.27–291.82	(Guo et al., 2021)
China	Steel slag	1.36	(Liu et al., 2018a)
China	Alkaline solid wastes	10.91–30	(Ma et al., 2022)

To further illustrate the function of lime as a carbon sink, the results obtained in the present study were compared with data for the uptake of CO₂ by materials containing different minerals (Table 2). Rocks containing silicate and carbonate minerals are abundant in nature and are continuously extracting CO₂ from the atmosphere. According to recent studies, the annual average amounts of carbon sequestered by natural carbonate and silicate minerals are 3.26890 and 34.64043 Mt C yr⁻¹Gt⁻¹yr⁻¹ (Li et al., 2018; Zhang et al., 2021). However, the weathering of these minerals resulting in sequestration of CO₂ from the atmosphere occurs over a timescale of at least 10⁴ years (Berner et al., 1983).

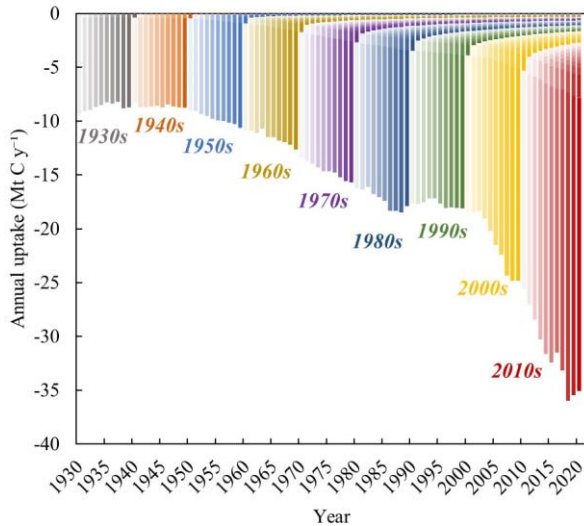


Figure 6: Worldwide annual uptake of atmospheric CO₂ by lime, disaggregated by years of production

Obviously, compared to natural carbonate and silicate minerals, the carbonation process involving alkaline materials produced by human activities, such as cement, SS and other solid wastes, is relatively faster under natural conditions (Berner et al.,

设置了格式: 字体颜色: 红色

设置了格式: 字体颜色: 红色, 上标

设置了格式: 字体颜色: 红色

设置了格式: 字体颜色: 红色, 突出显示

设置了格式: 字体颜色: 红色

设置了格式: 字体颜色: 红色, 突出显示

设置了格式: 字体颜色: 红色

设置了格式: 字体颜色: 红色, 突出显示

设置了格式: 字体颜色: 红色

设置了格式: 字体颜色: 红色, 突出显示

设置了格式: 字体颜色: 红色

设置了格式: 字体颜色: 红色, 突出显示

设置了格式: 字体颜色: 红色

设置了格式: 字体颜色: 红色, 突出显示

设置了格式: 字体颜色: 红色

设置了格式: 字体颜色: 红色, 突出显示

设置了格式: 上标

设置了格式: 字体: 加粗

设置了格式: 字体: (默认) Times New Roman, (中文) Times New Roman, 10 磅, 加粗, 字体颜色: 红色, 英语(英国)

设置了格式: 字体: 加粗

设置了格式: 字体: (默认) Times New Roman, (中文) Times New Roman, 10 磅, 加粗, 字体颜色: 红色, 英语(英国)

设置了格式: 字体: 加粗, 字体颜色: 红色

1983). Lime materials, such as MOR and SS, similar to cement and natural materials, also ~~serve for the removal~~ of CO₂ from the atmosphere for several years or decades (Fig. 56). ~~Alternatively, (The uptake of CO₂ in each year involves includes lime materials that were generated or consumed in previous and current years: the former accounts for 17-15.59%% of the total uptake, whereas the latter represents accounts for 834.41%%. These results contrast with those obtained for the cement carbon sink. These results are inconsistent with those obtained for the cement carbon sink,~~ where most of the carbon absorption is linked to previous years. This difference is attributed to the higher calcium content, smaller particle size, and more active chemical properties of lime materials. These characteristics suggest that lime-containing materials, especially LKD and SS, are suitable for carbon capture and storage via mineralisation. Therefore, promoting the carbonation process can mitigate impacts of CO₂ emissions (Pan et al., 2020).

5. Data availability

All the original datasets of CO₂ uptake by lime are available at <https://doi.org/10.5281/zenodo.7628614> <https://doi.org/10.5281/zenodo.7112485> (Ma et al., 2022). This dataset contains three data files, including lime material production and uses, lime carbon emission and uptake results, and the uncertainty of lime carbon emission and uptake.

6. Conclusion

In the present study, a carbon sequestration model was utilized to quantify the global uptake of CO₂ by lime-containing materials from 1930 to 2020. The national greenhouse gas inventories guideline methods and carbon budgets can be improved by considering lime as a carbon sink. The main findings of the present study are summarised below. Global CO₂ uptake from lime production processes increased from 9.16 Mt C yr⁻¹ in 1930 to 35.27 Mt C yr⁻¹ in 2020. However, the cumulative uptake of CO₂ by lime-containing materials (1444.70 Mt C) offset approximately 38.83% of these emissions. The uptake was highest in China (918.41 Mt C; 63.95% of global total) because of the associated elevated production and consumption of lime in recent decades. Uptake in the ROW and U.S. was 474.35 and 43.28 Mt C, respectively. The uptake of CO₂ by lime-containing materials varied significantly at different stages of the lime cycle. In the utilisation stage, lime-containing materials, especially LSS and MOR, contributed the most to the total lime carbon sink (1076.97 Mt C). This was followed by sequestration in lime materials (mainly SS and CS) during the waste disposal stage (299.19 Mt C), whereas the production stage was associated with 36.95 Mt C. Historically, weathering of lime-containing materials was thought to occur over a large timescale. In the present study, it was revealed that approximately 15.59% of the annual uptake of CO₂ originated from lime that was produced in previous decades;

设置了格式: 字体颜色: 红色

设置了格式: 字体颜色: 红色

设置了格式: 字体颜色: 红色

设置了格式: 字体颜色: 红色

设置了格式: 字体颜色: 红色

设置了格式: 字体颜色: 红色

设置了格式: 字体颜色: 红色

带格式的: 标题 1

therefore, this absorption potential cannot be ignored. In the future, carbon capture and storage can be improved via the use of lime-containing materials (e.g., SS and LKD).

In the present study, a carbon sequestration model was utilized to quantify the global uptake of CO₂ by lime-containing materials from 1963 to 2020. The national greenhouse gas inventories guideline methods and carbon budgets can be improved by considering lime as a carbon sink. The main findings of the present study are summarised below:

Global CO₂ uptake from lime production processes increased from 38.25 Mt yr⁻¹ in 1963 to 134.33 Mt yr⁻¹ in 2020. However, the cumulative uptake of CO₂ by lime-containing materials (4053.61 Mt) did offset approximately 25.82% of these emissions. The uptake was highest in China (2542.94 Mt) because of the associated elevated production and consumption of lime in recent decades, and this accounted for > 63.12% of the global uptake. Uptakes in the ROW and U.S. were 1358.23 and 127.41 Mt, respectively.

The uptake of CO₂ by lime-containing materials at different stages of its cycle varied significantly. In the utilisation stage, lime-containing materials, especially lime stabilised soil and lime mortar, contributed the most to the total lime carbon sink (2922.66 Mt). This was followed by sequestration in lime materials (mainly steel slag and carbide slag) in the waste disposal stage (933.61 Mt), whereas the production stage was associated with 101.66 Mt.

Historically, weathering of lime-containing materials was thought to occur over a large timescale. In the present study, it was revealed that approximately 17% of the annual uptake of CO₂ originated from lime that was produced in previous decades; therefore, this absorption potential cannot be ignored. In the future, carbon capture and storage can be improved via the use of lime-containing materials (e.g., steel slag and lime kiln dust).

Author contributions. LB and MM designed the study and prepared the manuscript with assistance from FX, JW, and LL. LL and MM performed the analyses, with the help of FX and LB on the analytical approaches. MM, LN, and FC performed the post-processing and analysis of the data as well as the review of the paper. LL and LB established the lime carbon sink accounting database, whereas LB and FX wrote the code and performed simulations of the datasets, with assistance from LL, MM, and LN. FX conceptualised and supervised the study.

Competing interests. The authors declare that they have no conflict of interest.

Acknowledgements. Longfei Bing, Mingjing Ma, and Fengming Xi acknowledge funding from the National Natural Science Foundation of China (No. 41977290), CAS President's International Fellowship Initiative (2017VCB0004), Youth Innovation Promotion Association, Chinese Academy of Sciences (grant nos. 2020201 and Y202050), Liaoning Xingliao Talents Project (No. XLYC1907148), and Natural Science Foundation of Liaoning Province (2021-MS-025).

Financial support. This research was funded by the National Natural Science Foundation of China (No. 41977290), CAS President's International Fellowship Initiative (2017VCB0004), Youth Innovation Promotion Association, Chinese Academy of Sciences (grant nos. 2020201 and Y202050), Liaoning Xingliao Talents Project (No. XLYC1907148), and Natural Science Foundation of Liaoning Province (2021-MS-025).

References

520 Baciocchi, R.: Carbonation of Industrial Residues for CCUS: Fundamentals, Energy Requirements and Scale-up Opportunities, CO₂ Summit III: Pathways to Carbon Capture, Utilization, and Storage Deployment, 2017.

Berner, R. A., Lasaga, A. C., and Garrels, R. M.: The carbonate-silicate geochemical cycle and its effect on atmospheric carbon dioxide over the past 100 million years., *American Journal of Science*, 283, 641–683, <https://doi.org/10.2475/AJS.283.7.641>, 1983.

525 Bhatia, S. and Perlmutter, D.: Effect of the product layer on the kinetics of the CO₂-lime reaction, *AIChE Journal*, 29, 79–86, <https://doi.org/10.1002/AIC.690290111>, 1983.

Bobicki, E. R., Liu, Q., Xu, Z., and Zeng, H.: Carbon capture and storage using alkaline industrial wastes, *Progress in Energy and Combustion Science*, 38, 302–320, <https://doi.org/10.1016/J.PECS.2011.11.002>, 2012.

530 Cao Z, Liu G, Duan H, Xi F, Yang Y; Unravelling the mystery of Chinese building lifetime: A calibration and verification based on dynamic material flow analysis. *Applied energy*, 238: 442-452. <https://doi.org/10.1016/j.apenergy.2019.01.106>, 2019.

China Construction Material Industry Yearbook. <https://data.cnki.net/yearBook/single?id=N2022040143>, 2022.

Cizer, Ö., Rodriguez-Navarro, C., Ruiz-Agudo, E., Elsen, J., van Gemert, D., and van Balen, K.: Phase and morphology evolution of calcium carbonate precipitated by carbonation of hydrated lime, *Journal of Materials Science*, 47, 6151–6165, <https://doi.org/10.1007/S10853-012-6535-7/FIGURES/9>, 2012a.

535 Cizer, Ö., van Balen, K., Elsen, J., and van Gemert, D.: Real-time investigation of reaction rate and mineral phase modifications of lime carbonation, *Construction and Building Materials*, 35, 741–751, <https://doi.org/10.1016/J.CONBUILDMAT.2012.04.036>, 2012b.

Cui, D., Deng, Z., and Liu, Z.: China’s non-fossil fuel CO₂ emissions from industrial processes, *Applied Energy*, 254, 113537, <https://doi.org/10.1016/J.APENERGY.2019.113537>, 2019.

540 Despotou, E., Shtiza, A., Schlegel, T., and Verhelst, F.: Literature study on the rate and mechanism of carbonation of lime in mortars / Literaturstudie über Mechanismus und Grad der Karbonatisierung von Kalkhydrat im Mörtel, *Mauerwerk*, 20, 124–137, <https://doi.org/10.1002/DAMA.201500674>, 2016.

Dong, Y., Yupin, W., Wang, W., and Dehai, L.: Demonstration Analysis of Chinese Construction Industry Output under Global Financial Crisis, *Science and Technology Management Research*, 72–75, 2010.

545 Almanac of China building materials industry: <https://data.oversea.cnki.net/chn/Trade/yearbook/single/N2021060085?zcode=Z005>, last access: 27 May 2022.

Data supplement to the Global Carbon Budget 2021: https://meta.icos-cp.eu/collections/88n-9-M7vk8jkXShAKj0RVL_, last access: 27 May 2022.

550 Greco-Coppi, M., Hofmann, C., Ströhle, J., Walter, D., and Epple, B.: Efficient CO₂ capture from lime production by an indirectly heated carbonate looping process, *International Journal of Greenhouse Gas Control*, 112, 103430, <https://doi.org/10.1016/J.IJGGC.2021.103430>, 2021.

带格式的：两端对齐

设置了格式：下标

设置了格式：下标

设置了格式：字体：(默认) Times New Roman, 字体颜色：红色, 图案：清除

设置了格式：字体颜色：红色

设置了格式：字体：(默认) Times New Roman, 字体颜色：红色, 图案：清除

设置了格式：默认段落字体, 字体颜色：红色

设置了格式：字体：Times New Roman, 10磅, 字体颜色：红色, 图案：清除

设置了格式：字体颜色：红色

设置了格式：默认段落字体, 字体颜色：红色

设置了格式：字体颜色：红色

设置了格式：下标

设置了格式：下标

- Guo, R., Wang, J., Bing, L., Tong, D., Ciais, P., Davis, S. J., Andrew, R. M., Xi, F., and Liu, Z.: Global CO₂ uptake by cement from 1930 to 2019, *Earth System Science Data*, 13, 1791–1805, <https://doi.org/doi.org/10.5194/essd-13-1791-2021>, 2021.
- 555 Hao, J., Jiang, X., Yang, H., Yang, S., and Li, zhaoliang: Research Progress and Application of Carbide Slag, *Guangzhou Chemical Industry*, 41, 45–46, 2013.
- Huang, C., Deng, Y., Xing, X., and Lu, J.: Comprehensive utilization of carbide slag, *Journal of Jiaozuo Institute of Technology (Natural Science)*, 23, 143–146, 2004.
- Intergovernmental Panel on Climate Change. IPCC guidelines for national greenhouse gas inventories. Hayama (Japan): Institute for Global Environmental Strategies (IGES); 2006.
- 560 Lai, Q. T., Habte, L., Thriveni, T., Seongho, L., and Ahn, J. W.: COVID-19 Impacts on Climate Change—Sustainable Technologies for Carbon Capture Storage and Utilization (CCUS), *Minerals, Metals and Materials Series*, 23–28, https://doi.org/10.1007/978-3-030-65257-9_3/FIGURES/3, 2021.
- Latif, M. A., Naganathan, S., Razak, H. A., and Mustapha, K. N.: Performance of Lime Kiln Dust as Cementitious Material, *Procedia Engineering*, 125, 780–787, <https://doi.org/10.1016/J.PROENG.2015.11.135>, 2015.
- 565 Li, H., Wang, S., Bai, X., Luo, W., Tang, H., Cao, Y., Wu, L., Chen, F., Li, Q., Zeng, C., and Wang, M.: Spatiotemporal distribution and national measurement of the global carbonate carbon sink, *Science of The Total Environment*, 643, 157–170, <https://doi.org/https://doi.org/10.1016/j.scitotenv.2018.06.196>, 2018.
- Lin, Q., Wang, X., Cao, J., and Zhang, J.: Preparation of Nanosized Calcium Carbonate from Calcium Carbide Residue, *Guizhou Chemical Industry*, 3, 5–7, 2006.
- 570 Liu, L., Wang, J., Bing, L., Ling, J., Xu, M., and Xi, F.: Analysis of carbon sink of steel slag in China, *Chinese Journal of Applied Ecology*, 29, 3385–3390, 2018a.
- Liu, L. L., Ling, J. H., Li, T., Wang, J. Y., and Xi, F. M.: Review of lime carbon sink, *Chinese Journal of Applied Ecology*, 29, 327–334, 2018b.
- Ma, J., Chen, Y., Xu, D., Xu, F., Xue, S., Fan, B., Liu, D. kuan, and Ma, S.: Effects of Particle Size difference between White Mud and Limestone on Desulfurization Performance, *Journal of Chinese Society of Power Engineering*, 6, 497–504, 2021.
- 575 Ma, M. J., Ma, M. J., Xi, F. M., Ling, J. H., Ling, J. H., Wang, J. Y., and Quan, S. M.: Research progress cm mineral carbonation of carbon dioxide, *Chinese Journal of Ecology*, 38, 3854–3863, <https://doi.org/10.13292/J.1000-4890.201912.002>, 2019.
- China Statistical Yearbook: <https://data.stats.gov.cn/easyquery.htm?cn=C01>, last access: 27 May 2022.
- China Chemical Industry Yearbook: <https://data.cnki.net/Trade/yearbook/single/N2021010132?zcode=Z023>, last access: 27
- 580 May 2022.
- National Lime Association: RE: Comments of the National Lime Association on: Increasing Consistency and Transparency in Considering Benefits and Costs in the Clean Air Act Rulemaking Process, 2020.
- NOAA. ESRL: Global Monitoring Division—Global Greenhouse Gas Reference Network, n.d.

- 585 [Pan, S. Y., Chen, Y. H., Fan, L. S., Kim, H., Gao, X., Ling, T. C., Chiang, P. C., Pei, S. L., and Gu, G.: CO₂ mineralization and utilization by alkaline solid wastes for potential carbon reduction, *Nature Sustainability*, 3, 399–405, <https://doi.org/10.1038/s41893-020-0486-9>, 2020.](#)
- Pan, S.-Y., Chang, E. E., and Chiang, P.-C.: CO₂ capture by accelerated carbonation of alkaline wastes: a review on its principles and applications, *Aerosol and Air Quality Research*, 12, 770–791, 2012.
- 590 **PR China National Development and Reform Commission. Guidelines for provincial greenhouse gas inventories; 2011. [Chinese Document].**
- Qin, J., Cui, C., Cui, X., Hussain, A., Yang, C., and Yang, S.: Recycling of lime mud and fly ash for fabrication of anorthite ceramic at low sintering temperature, *Ceramics International*, 41, 5648–5655, <https://doi.org/10.1016/J.CERAMINT.2014.12.149>, 2015.
- Renforth, P.: The negative emission potential of alkaline materials, *Nature Communications*, 10, 1–8, <https://doi.org/10.1038/s41467-019-09475-5>, 2019.
- 595 Samari, M., Ridha, F., Manovic, V., Macchi, A., and Anthony, E. J.: Direct capture of carbon dioxide from air via lime-based sorbents, *Mitigation and Adaptation Strategies for Global Change*, 25, 25–41, <https://doi.org/10.1007/S11027-019-9845-0>/FIGURES/7, 2020.
- 600 [Shan, Y., Liu, Z., and Guan, D.: CO₂ emissions from China's lime industry, *Applied Energy*, 166, 245–252, <https://doi.org/10.1016/j.apenergy.2015.04.091>, 2016a.](#)
- ~~Shan, Y., Liu, Z., and Guan, D.: CO₂ emissions from China's lime industry, *Applied Energy*, 166, 245–252, <https://doi.org/10.1016/j.apenergy.2015.04.091>, 2016b.~~
- 605 Snæbjörnsdóttir, S., Sigfússon, B., Marieni, C., Goldberg, D., Gislason, S. R., and Oelkers, E. H.: Carbon dioxide storage through mineral carbonation, *Nature Reviews Earth & Environment* 2020 1:2, 1, 90–102, <https://doi.org/10.1038/s43017-019-0011-8>, 2020.
- Tong, Q., Zhou, S., Guo, Y., Zhang, Y., and Wei, X.: Forecast and Analysis on Reducing China's CO₂ Emissions from Lime Industrial Process, *Int J Environ Res Public Health*, 16, <https://doi.org/10.3390/IJERPH16030500>, 2019.
- Iron and Steel Slag, [U.S. Geological Survey](#): <https://pubs.usgs.gov/periodicals/mcs2021/mcs2021-iron-steel-slag.pdf>, last access: 27 May 2022.
- 610 Lime Statistics and Information+, [U.S. Geological Survey](#): <https://www.usgs.gov/centers/national-minerals-information-center/lime-statistics-and-information>, last access: 26 May 2022.
- Ventol, L., Vendrell, M., Giraldez, P., and Merino, L.: Traditional organic additives improve lime mortars: New old materials for restoration and building natural stone fabrics, *Construction and Building Materials*, 25, 3313–3318, <https://doi.org/10.1016/J.CONBUILDMAT.2011.03.020>, 2011.
- 615 Wang, L., Sun, N., Tang, H., and Sun, W.: A review on comprehensive utilization of red mud and prospect analysis, *Minerals*, 9, <https://doi.org/10.3390/MIN9060362>, 2019.

设置了格式: 字体颜色: 红色

设置了格式: 字体颜色: 红色, 下标

设置了格式: 字体颜色: 红色

设置了格式: 字体颜色: 红色

设置了格式: 字体颜色: 红色, 下标

设置了格式: 字体颜色: 红色

Wang, Q. and Yan, P.: Characteristic of hydration products of steel slag, *Journal of the Chinese Ceramic society*, 38, 1731–1734, <https://doi.org/10.14062/j.issn.0454-5648.2010.09.030>, 2010.

620 Xi, F., Davis, S. J., Ciaia, P., Crawford-Brown, D., Guan, D., Pade, C., Shi, T., Syddall, M., Lv, J., Ji, L., Bing, L., Wang, J., Wei, W., Yang, K. H., Lagerblad, B., Galan, I., Andrade, C., Zhang, Y., and Liu, Z.: Substantial global carbon uptake by cement carbonation, *Nature Geoscience*, 9, 880–883, <https://doi.org/10.1038/ngeo2840>, 2016.

Zhang, S., Bai, X., Zhao, C., Tan, Q., Luo, G., Wang, J., Li, Q., Wu, L., Chen, F., Li, C., Deng, Y., Yang, Y., and Xi, H.: Global CO₂ Consumption by Silicate Rock Chemical Weathering: Its Past and Future, *Earth's Future*, 9, <https://doi.org/10.1029/2020EF001938>, 2021.

625

设置了格式: 下标

Figure captions

带格式的: 左, 缩进: 左侧: 0.35 厘米, 右侧: 0.35 厘米, 行距: 单倍行距

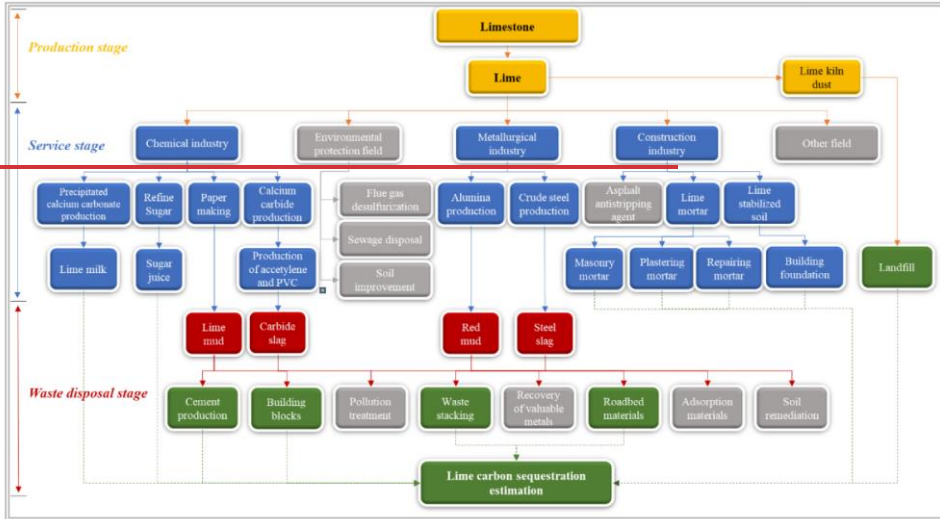
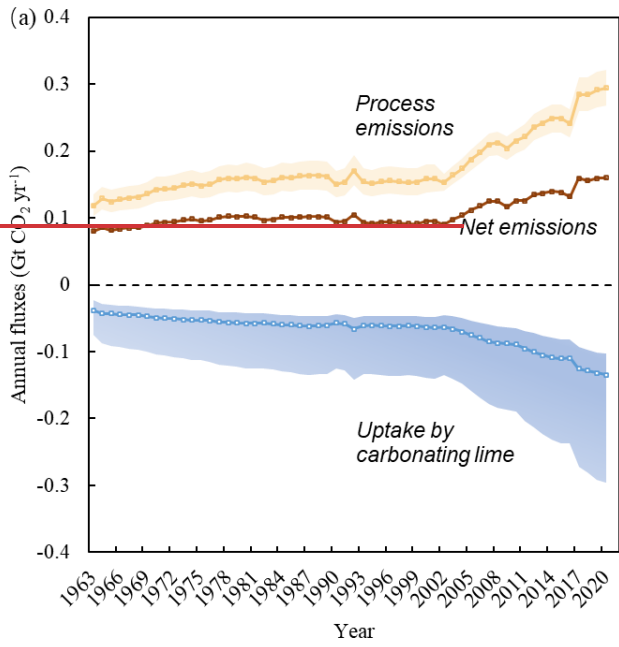


Figure 1: System boundary for the sequestration of carbon by lime. Solid arrows represent the material flow, whereas dashed arrows indicate the carbon flow, and the double solid lines are accounting boundaries.

630



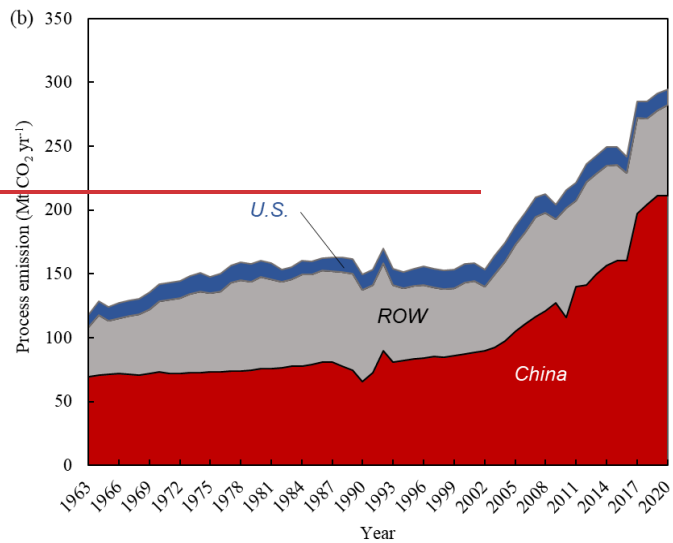
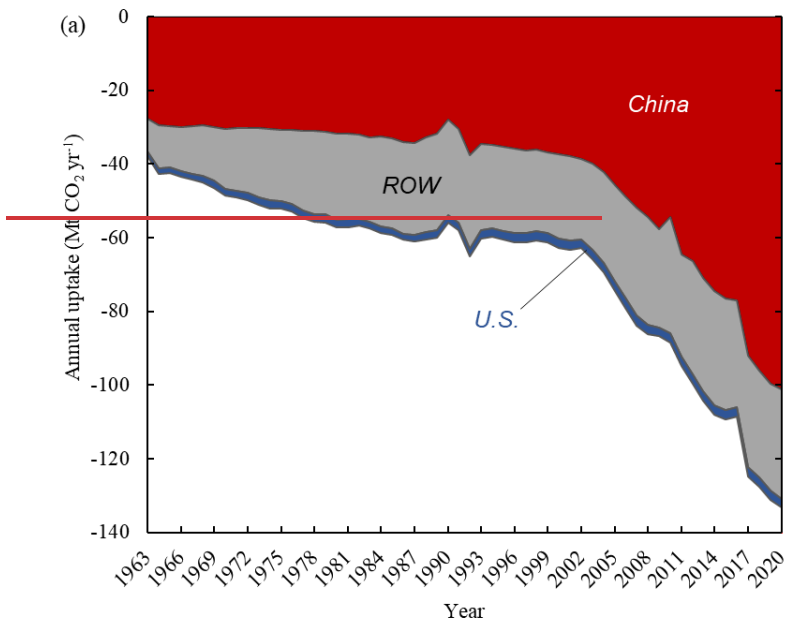
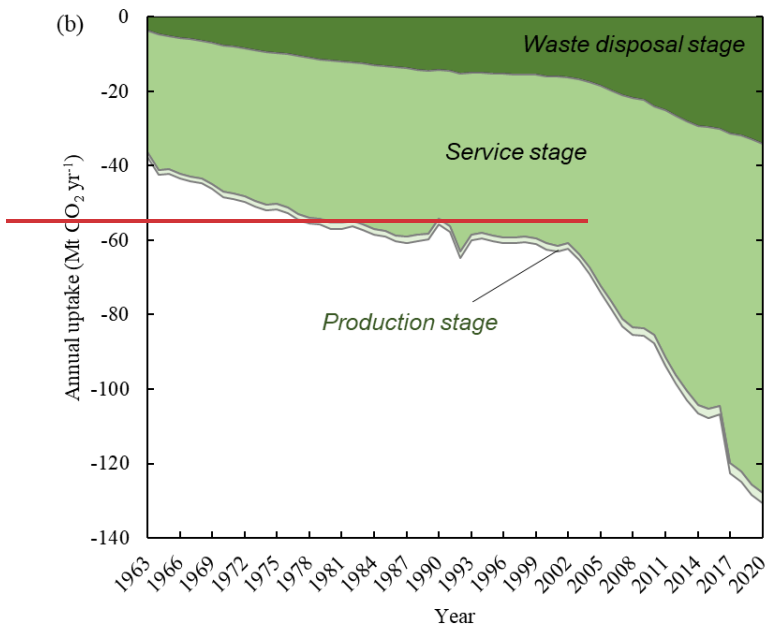


Figure 2: (a) Annual CO₂ emissions from industrial processes and the associated uptake by lime from 1963 to 2020. Shadows represent uncertainty ranges. (b) Country- and region-wise CO₂ emissions (median) generated by industrial processes from 1963 to 2020. ROW (Rest of World).

635





640

Figure 3: Annual uptake of carbon dioxide by lime (a) in different regions and (b) during different stages of its cycle. ROW (Rest of World)

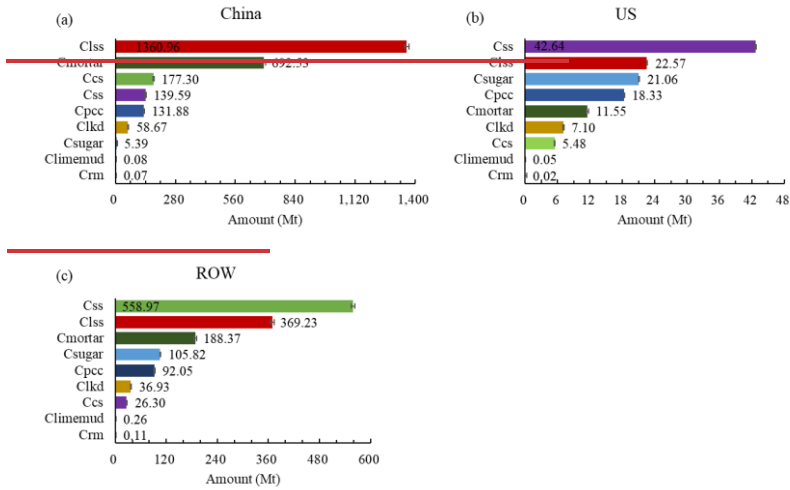


Figure 4: Cumulative uptake of CO₂ uptake by lime-containing materials in different regions. ROW (Rest of World, ROW (Rest of World), Ces (CO₂ uptake by carbide slag), Clkd (CO₂ uptake by lime kiln dust), Clss (CO₂ uptake by lime stabilised soil), Cmor (CO₂ uptake by lime mortar), Cpcc (CO₂ uptake by Precipitated calcium carbonate), Crm (CO₂ uptake by red mud), Ccs (CO₂ uptake by steel slag), Csug (CO₂ uptake by carbonation sugar), Clm (CO₂ uptake by lime mud).

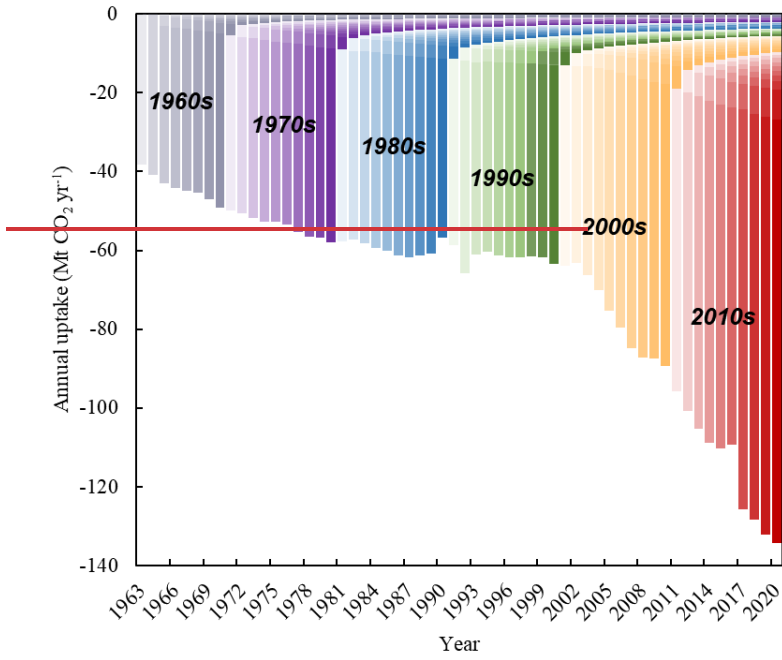


Figure 5: Cumulative uptake of CO₂ by lime from 1963 to 2020.

655

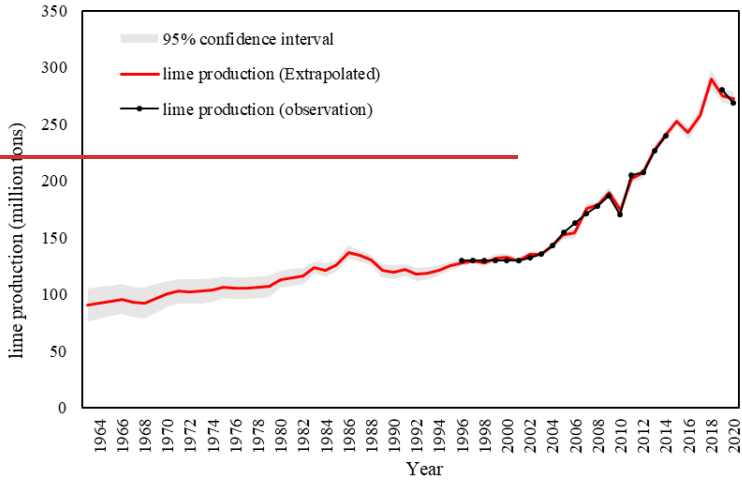


Figure 6. China's lime production estimation in 1963-2020

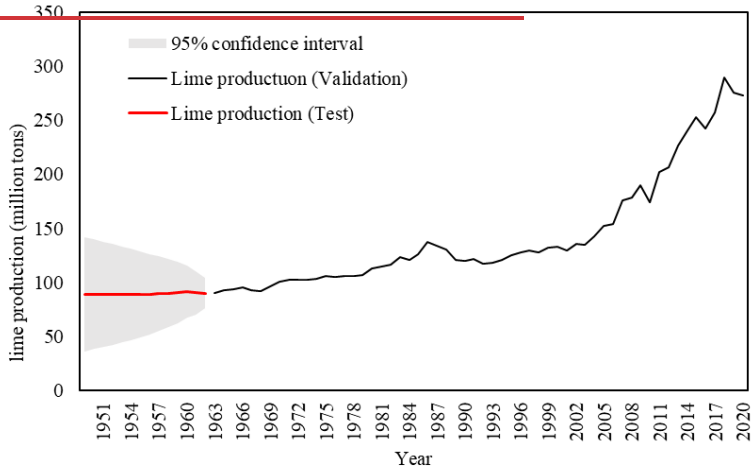


Figure 7. China's lime production estimation in 1949-1962

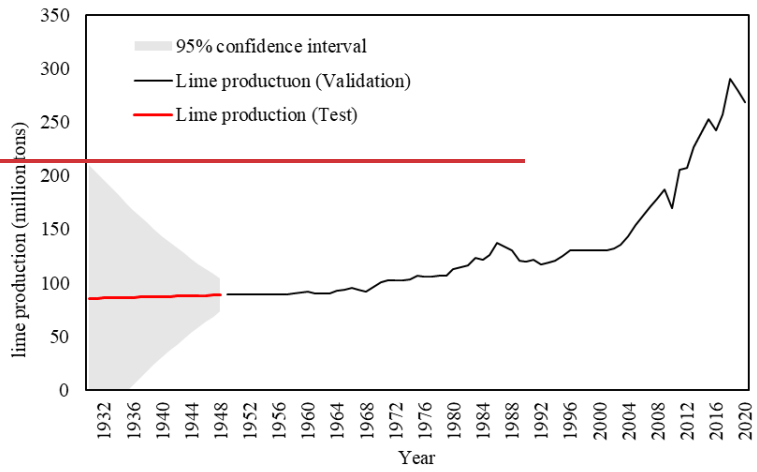


Figure 8. China's lime production estimation in 1930-1948

660

Table 1. Summary of the global uptake of CO₂ by lime-containing materials in different stages of its cycle

Stage	Types of lime materials	CO ₂ uptake in 2020 (Mt)	Cumulative CO ₂ uptake from 1963 to 2020 (Mt)
Production	LKD	2.95	101.66
	LSS	57.03	1729.04
Service	MOR	27.51	834.77
	PCC	6.70	233.30
	SUG	2.43	125.54
Waste disposal	RM	0.01	0.15
	SS	27.34	721.33
	CS	6.84	200.84
	LM	0.01	0.29

LKD(Lime Kiln Dust), LSS (Lime Stabilised Soil), PCC (Precipitated Calcium Carbonate), SUG (Carbonation Sugar), RM (Red Mud), SS (Steel Slag), CS (Carbide Slag), LM (Lime Mud)

Table 2. Comparison of CO₂ uptake by different types of materials

Region	Carbon sink type	Annual CO ₂ uptake (Gt/yr)	Source
Global	Carbonate	2.42–4.11	(Li et al., 2018)
Global	Silicate	0.13	(Zhang et al., 2021)
Global	Lime	0.09–0.19	this study
Global	Cement	0.89	(Guo et al., 2021)
China	Steel slag	0.005	(Liu et al., 2018a)
China	Alkaline solid wastes	0.04–0.11	(Ma et al., 2022)

A gigatonne (Gt) is 1,000,000,000 tonnes

665